JACS
JOURNAL OF THE AMERICAN CHEMICAL SOCIETY
Article
pubs.acs.org/JACS

Enhanced Electron-Transfer Reactivity of Nonheme Manganese(IV)−Oxo Complexes by Binding Scandium Ions

Heejung Yoon,[†,‡] Yong-Min Lee,[‡] Xiujuan Wu,[‡] Kyung-Bin Cho,[‡] Ritimukta Sarangi,[§] Wonwoo Nam,*[,‡] and Shunichi Fuhkuzumi*[,†,‡]

[†]Department of Material and Life Science, Graduate School of Engineering, ALCA, Japan Science and Technology Agency (JST), Osaka University, Suita, Osaka 565-0871, Japan

[‡]Department of Bioinspired Science, Ewha Womans University, Seoul 120-750, Korea

[§]Stanford Synchrotron Radiation Lightsource, SLAC National Accelerator Laboratory, Menlo Park, California 94025, United States

Supporting Information

ABSTRACT: One and two scandium ions (Sc^{3+}) are bound strongly to nonheme manganese(IV)−oxo complexes, $[(N4Py)Mn^{IV}(O)]^{2+}$ (N4Py = *N*,*N*-bis(2-pyridylmethyl)-*N*-bis(2-pyridyl)methylamine) and $[(Bn\text{-}TPEN)Mn^{IV}(O)]^{2+}$ (Bn-TPEN = *N*-benzyl-*N*,*N*′,*N*′-tris(2-pyridylmethyl)-1,2-diaminoethane), to form $Mn^{IV}(O)-(Sc^{3+})_1$ and $Mn^{IV}(O)-(Sc^{3+})_2$ complexes, respectively. The binding of Sc^{3+} ions to the $Mn^{IV}(O)$ complexes was examined by spectroscopic methods as well as by DFT calculations. The one-electron reduction potentials of the $Mn^{IV}(O)$ complexes were markedly shifted to a positive direction by binding of Sc^{3+} ions. Accordingly, rates of the electron transfer reactions of the $Mn^{IV}(O)$ complexes were enhanced as much as 10^7−fold by binding of two Sc^{3+} ions. The driving force dependence of electron transfer from various electron donors to the $Mn^{IV}(O)$ and $Mn^{IV}(O)-(Sc^{3+})_2$ complexes was examined and analyzed in light of the Marcus theory of electron transfer to determine the reorganization energies of electron transfer. The smaller reorganization energies and much more positive reduction potentials of the $Mn^{IV}(O)-(Sc^{3+})_2$ complexes resulted in remarkable enhancement of the electron-transfer reactivity of the $Mn^{IV}(O)$ complexes. Such a dramatic enhancement of the electron-transfer reactivity of the $Mn^{IV}(O)$ complexes by binding of Sc^{3+} ions resulted in the change of mechanism in the sulfoxidation of thioanisoles by $Mn^{IV}(O)$ complexes from a direct oxygen atom transfer pathway without metal ion binding to an electron-transfer pathway with binding of Sc^{3+} ions.

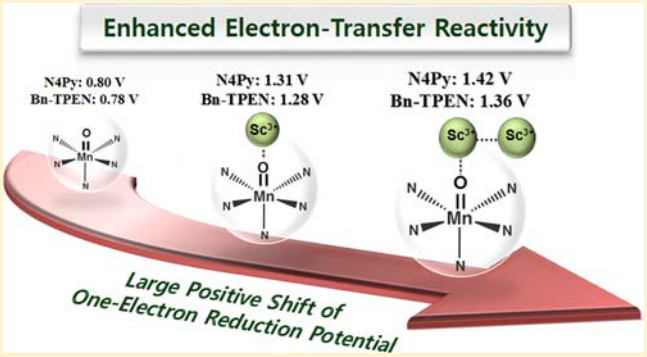

INTRODUCTION

High-valent metal−oxo complexes play pivotal roles as reactive intermediates in the reactions of heme (cytochromes P450 and peroxidases)[1−3] and nonheme metalloenzymes (taurine/α-ketoglutarate dioxygenase (TauD),[4] soluble methane monooxygenase (sMMO),[5] and oxygen-evolving center (OEC) in Photosystem II[6,7]) as well as in their biomimetic oxidation catalysis.[8−13] A number of synthetic high-valent metal−oxo complexes have been synthesized and characterized by various spectroscopic techniques as well as by X-ray crystallography.[8−17] The oxidizing reactivity of the high-valent metal−oxo complexes has so far been finely controlled by the oxidation state of metals and the supporting and axial ligands.[8−28] Alternatively, binding of redox-inactive metal ions acting as Lewis acids to the metal−oxo moiety of high-valent metal−oxo complexes has also been reported to enhance the oxidizing power of the metal−oxo complexes.[29−32] For example, Lau and co-workers have shown that rates of oxidation of alkanes by MnO_4^- are accelerated dramatically by addition of Lewis acids.[33] We have reported the first X-ray crystal structure of a Sc^{3+} ion-bound iron(IV)−oxo complex[34] and found that the binding of Sc^{3+} ions to iron(IV)−oxo complexes resulted in the remarkable enhancement of the oxidizing reactivity of the iron−oxo complexes in various oxidation reactions.[29] Those findings are reminiscent of the indispensable role of Ca^{2+} in the manganese−oxo-calcium (Mn_4CaO_5) active site in OEC, which catalyzes four-electron oxidation of water to dioxygen, although the exact function of Ca^{2+} has yet to be clarified.[35,36] In this context, we have recently communicated preliminary results that binding of redox-inactive metal ions to a nonheme manganese(IV)−oxo complex affected the oxidizing ability significantly.[37] Goldberg and co-workers also reported the influence of a redox-inactive Zn^{2+} ion on a valence tautomerization of a manganese(V)−oxo corrolazine complex.[38] More recently, Agapie and co-workers reported that the redox potentials of tetranuclear heterometallic trimanganese dioxo clusters $[Mn_3M(\mu_4\text{-}O)(\mu_2\text{-}O)]$ containing a redox-

Received: April 22, 2013
Published: June 6, 2013

   dx.doi.org/10.1021/ja403965h | J. Am. Chem. Soc. 2013, 135, 9186−9194

inactive metal ion, which were synthesized as an excellent structural model of the OEC active site,[39] were systematically controlled by the Lewis acidity of the redox-inactive metal ions.[40] The positive shift in the redox potentials of an iron(IV)−oxo complex was also observed in the presence of various redox-inactive metal ions, showing a correlation between the reactivity of the iron(IV)−oxo complex and the Lewis acidity of the redox-inactive metal ions.[29a] However, the electron-transfer properties of metal ion-bound manganese(IV)−oxo ($Mn^{IV}(O)$) complexes, which are the most fundamental factor in controlling the reactivity of metal−oxo species in oxidation reactions, have yet to be clarified.

We report herein not only the synthesis and characterization of nonheme $Mn^{IV}(O)$ complexes binding one and two Sc^{3+} ions, $Mn^{IV}(O)-(Sc^{3+})_1$ and $Mn^{IV}(O)-(Sc^{3+})_2$, but also the detailed kinetic data on electron transfer from various electron donors to $Mn^{IV}(O)$, $Mn^{IV}(O)-(Sc^{3+})_1$, and $Mn^{IV}(O)-(Sc^{3+})_2$ complexes. The large positive shifts in one-electron reduction potentials of $Mn^{IV}(O)$ complexes by binding of one and two Sc^{3+} ions have also been determined for the first time by carrying out redox titration experiments using electron donors with known one-electron oxidation potentials. Rates of the electron-transfer reactions by $Mn^{IV}(O)$ complexes were remarkably enhanced by binding of Sc^{3+} ions. The driving force dependence of the rate constants of electron-transfer reactions has been analyzed in light of the Marcus theory of electron transfer[41] to determine the reorganization energies of electron transfer of Sc^{3+} ion-bound $Mn^{IV}(O)$ complexes in comparison with those of $Mn^{IV}(O)$ complexes without Sc^{3+} ions. We have also shown that binding of redox-inactive metal ions enhances the reactivity of $Mn^{IV}(O)$ complexes in sulfoxidation of thioanisoles and changes the sulfoxidation mechanism from direct oxygen atom transfer to electron transfer.

RESULTS AND DISCUSSION

Binding of Sc^{3+} Ions to Nonheme $Mn^{IV}(O)$ Complexes. $[(Bn\text{-}TPEN)Mn^{IV}(O)]^{2+}$ (**1**) and its scandium-bound species were synthesized and characterized spectroscopically, as reported for binding of Sc^{3+} ions to $[(N4Py)Mn^{IV}(O)]^{2+}$ (**2**) (see Chart 1).[37,41] Addition of up to 2 equiv of $Sc(OTf)_3$ to a solution of **1** in a solvent mixture of CF_3CH_2OH/CH_3CN (v/v = 19:1) resulted in a blue shift of the absorption band of **1** at λ_{max} = 1020 nm to that at λ_{max} = 740 nm with an isosbestic point at 900 nm (Figure 1a). Such a blue shift suggests that the ground state of **1** is more stabilized by binding of Sc^{3+} ions. Further addition of $Sc(OTf)_3$ resulted in a more blue-shift to give the absorption band at λ_{max} = 690 nm (Figure 1c). No further spectral change was observed by addition of more than 9 equiv of $Sc(OTf)_3$. Such stepwise spectral changes indicate the binding of one and two Sc^{3+} ions to **1** to produce $Mn^{IV}(O)-(Sc^{3+})_1$ and $Mn^{IV}(O)-(Sc^{3+})_2$ complexes, respectively. The X-band EPR spectra of $[(Bn\text{-}TPEN)Mn^{IV}(O)]^{2+}-(Sc^{3+})_1$ and $[(Bn\text{-}TPEN)Mn^{IV}(O)]^{2+}-(Sc^{3+})_2$ exhibit signals that are characteristic of S = 3/2 Mn^{IV} (Figure S1 in Supporting Information (SI)). This result is the same as that reported previously for the complexes of **2** with Sc^{3+} ions.[37] The magnetic moments of $[(Bn\text{-}TPEN)Mn^{IV}(O)]^{2+}-(Sc^{3+})_1$ and $[(Bn\text{-}TPEN)Mn^{IV}(O)]^{2+}-(Sc^{3+})_2$ were also determined to be 4.4 and 4.3 μ_B by the modified NMR technique of Evans,[42] respectively, confirming the spin state of S = 3/2 for both complexes.[41a]

Chart 1

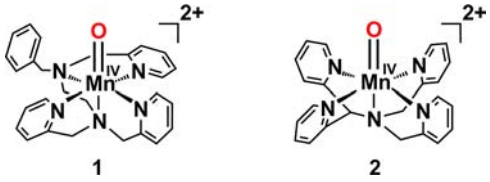

1 **2**

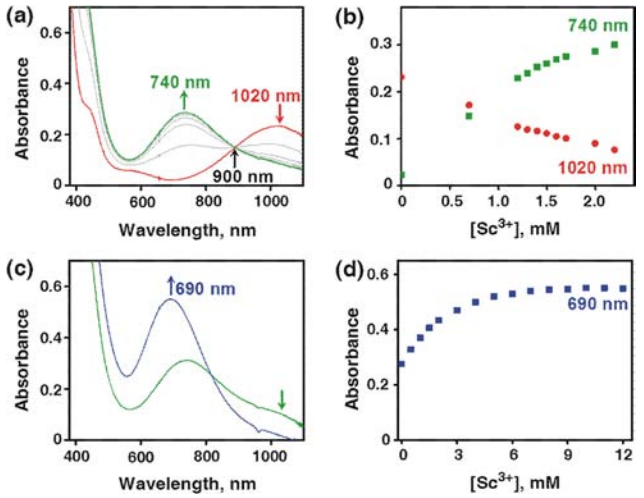

Figure 1. (a) UV−vis spectral changes showing the conversion from $[(Bn\text{-}TPEN)Mn^{IV}(O)]^{2+}$ (red line) to $[(Bn\text{-}TPEN)Mn^{IV}(O)]^{2+}-(Sc^{3+})_1$ (green line) upon addition of incremental amounts of Sc^{3+} (from 0.0 to 2.0 mM) in the titration experiment. (b) Spectroscopic titration monitored at 1020 nm (red rhombuses) due to the decay of $[(Bn\text{-}TPEN)Mn^{IV}(O)]^{2+}$ and at 740 nm (green squares) due to the formation of $[(Bn\text{-}TPEN)Mn^{IV}(O)]^{2+}-(Sc^{3+})_1$. (c) UV−vis spectral changes showing the conversion from $[(Bn\text{-}TPEN)Mn^{IV}(O)]^{2+}-(Sc^{3+})_1$ (green line) to $[(Bn\text{-}TPEN)Mn^{IV}(O)]^{2+}-(Sc^{3+})_2$ (blue line) observed upon addition of Sc^{3+} ions (from 0.0 to 12 mM). (d) Spectroscopic titration monitored at 690 nm (blue squares) due to $[(Bn\text{-}TPEN)Mn^{IV}(O)]^{2+}-(Sc^{3+})_2$.

The formation constant of the $[(Bn\text{-}TPEN)Mn^{IV}(O)]^{2+}-(Sc^{3+})_1$ complex was determined to be 4.0×10^3 M^{-1}, by analyzing the spectral change in Figure 1b (see the linear plot to determine the formation constant in Figure S2a in the SI).[43] The formation constant of the $[(Bn\text{-}TPEN)Mn^{IV}(O)]^{2+}-(Sc^{3+})_2$ complex was also determined to be 1.2×10^3 M^{-1} from the titration curve in Figure 1d (see also Figure S2b in SI for the linear plot to determine the formation constant), which is somewhat smaller than that of the $[(N4Py)Mn^{IV}(O)]^{2+}-(Sc^{3+})_2$ complex (6.1×10^3 M^{-1}).[37]

The structural details of Sc^{3+} binding was investigated using Mn K-edge EXAFS on **1**, $[(Bn\text{-}TPEN)Mn^{IV}(O)]^{2+}-(Sc^{3+})_1$ and $[(Bn\text{-}TPEN)Mn^{IV}(O)]^{2+}-(Sc^{3+})_2$ (see the SI, Experimental section for X-ray absorption spectroscopy, Figure S3 and Table S1). The EXAFS results show that on going from no Sc^{3+} binding in **1** to one and two Sc^{3+} binding, the Mn=O bond elongates from 1.69 to 1.74(2) Å, which is consistent with a weakening of the Mn=O bond. The EXAFS data also reveal a short Mn−Sc distance (3.45(10) Å), which clearly indicates that Sc^{3+} ions bind to the $Mn^{IV}(O)$ moiety in both $[(Bn\text{-}TPEN)Mn^{IV}(O)]^{2+}-(Sc^{3+})_1$ and $[(Bn\text{-}TPEN)Mn^{IV}(O)]^{2+}-(Sc^{3+})_2$.

Density functional theory (DFT)[44] calculations of the $Mn^{IV}(O)-(Sc^{3+})_2$ complex suggest that one Sc^{3+} ion binds

dx.doi.org/10.1021/ja403965h | J. Am. Chem. Soc. 2013, 135, 9186−9194

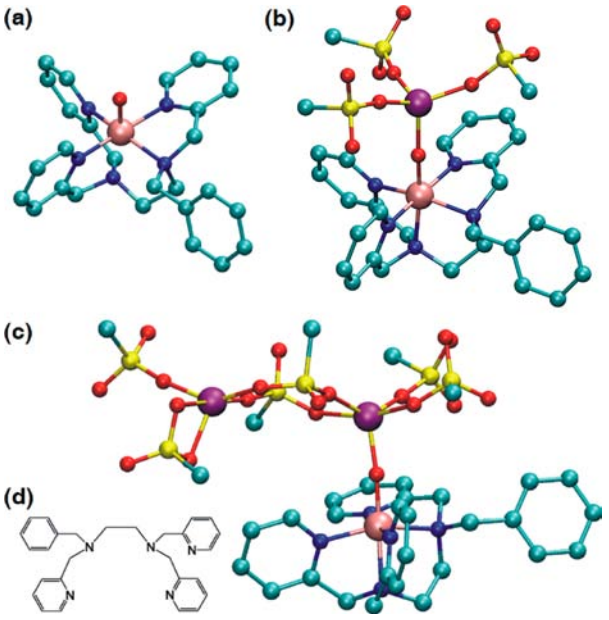

Figure 2. DFT-optimized structures of (a) $[(Bn\text{-}TPEN)Mn^{IV}(O)]^{2+}$ (**1**), (b) $[(Bn\text{-}TPEN)Mn^{IV}(O)-Sc(OTf)_3]^{2+}$, and (c) $[(Bn\text{-}TPEN)Mn^{IV}(O)-[Sc(OTf)_3]_2]^{2+}$, calculated at the B3LYP/LACVP level in the solvent phase. The Mn−O bond lengths of $[Mn^{IV}(O)]^{2+}$, $[Mn^{IV}(O)]^{2+}-Sc^{3+}$, and $[Mn^{IV}(O)]^{2+}-(Sc^{3+})_2$ were calculated to be 1.68, 1.75, and 1.75 Å, respectively (see the DFT Calculations Section in the the SI for computational details). H atoms in Bn-TPEN and F atoms in the OTf−counterions have been omitted for clarity (Mn, pink; N, blue; O, red; C, green; Sc, purple; S, yellow). (d) Schematic drawing of the Bn-TPEN ligand.

directly to the oxo moiety of the $Mn^{IV}(O)$ complex but the second Sc^{3+} ion is located at the secondary coordination sphere (see the DFT-optimized structures in Figure 2).[37,45] As shown previously, the Mn−O bond is elongated upon one Sc^{3+} binding (from 1.68 Å to 1.75 Å), but no further elongation is seen upon binding of the second Sc^{3+} ion (Table S2 in SI). This result is in a good agreement with that obtained from EXAFS experiments. This is also in line with what has been observed previously with $[(N4Py)Mn^{IV}(O)]^{2+}$ (**2**).[37] The significant blue shift in the absorption band of the $Mn^{IV}(O)-(Sc^{3+})_2$ complex as compared with that of the $Mn^{IV}(O)-(Sc^{3+})_1$ complex indicates that the electronic state of the $Mn^{IV}(O)$ moiety is somewhat perturbed by binding of the second Sc^{3+} ion, but the conservation of the core geometry in $Mn^{IV}(O)-(Sc^{3+})_2$, compared to $Mn^{IV}(O)-(Sc^{3+})_1$, suggests that the changes mostly affect the unoccupied virtual orbitals (such as σ^*_{xy}). The blue-shift indicates that the virtual orbitals are shifted higher in energy relative to HOMO, hence stabilizing the occupied orbitals.[46] The Mulliken spin density distribution shows negligible spin on the Sc^{3+} or counteranion atoms in all cases, while showing around three radicals in total for the Mn(O)-5xN moiety (Table S3 in the SI), indicating that the $Mn^{IV}(O)$ configuration is kept after Sc^{3+} binding. Indeed, natural orbital analysis showed that the valence orbital occupation was (δ, π^*_{xz}, and π^*_{yz}) corresponding to high-spin $Mn^{IV}(O)$. In addition, none of the nine valence $Mn^{IV}(O)$ orbitals with Mn d-orbital elements in it is mixing with Sc^{3+} orbitals, indicating a pure ionic $Mn^{IV}(O)-Sc^{3+}$ bond despite the short distance (1.94 Å). Hence, the $Mn^{IV}-O$ bond elongation can be attributed to pure Coulomb interactions rather than to changes in the electronic structure.

Positive Shifts in One-Electron Reduction Potentials of Nonheme $Mn^{IV}(O)$ Complexes by Binding of Sc^{3+} Ions. Electron transfer from ferrocene derivatives to $Mn^{IV}(O)$ complexes **1** and **2** occurred to completion in CF_3CH_2OH/CH_3CN (v/v = 1:1) at 273 K (Figure 3a). The solvent mixture

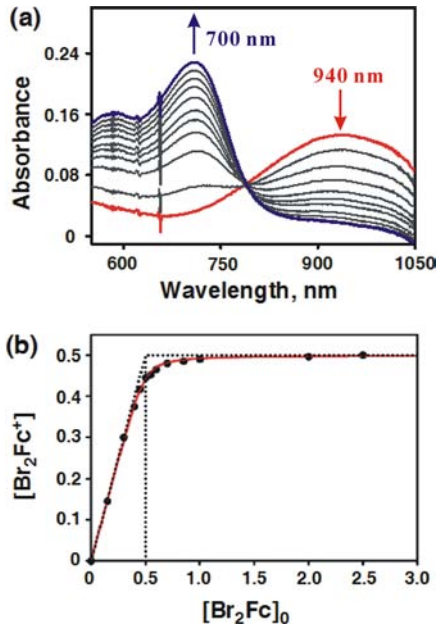

Figure 3. (a) Absorption spectral changes observed in electron transfer from dibromoferrocene (Br_2Fc; 5.0×10^{-3} M) to $[(N4Py)Mn^{IV}(O)]^{2+}$ (**2**; 5.0×10^{-4} M) in CF_3CH_2OH/CH_3CN (v/v = 1:1) at 273 K. (b) Plot of concentration of Br_2Fc^+ produced in electron transfer from Br_2Fc to **2** vs initial concentration of Br_2Fc, $[Br_2Fc]_0$.

was used due to the solubility of electron donors and the stability of **1** and **2**; both of which are quite stable at 273 K. The redox titration for formation of dibromoferrocenium ion (Br_2Fc^+) in Figure 3b indicates only one-electron reduction of **2** occurred without further reduction by Br_2Fc (see Table 1 for E_{ox} values of electron donors). This result is in agreement with the result of the redox titration of **1** with dibromoferrocene (Br_2Fc) reported previously.[41b]

When ferrocene derivatives were replaced by a weaker reductant such as $[Ru^{II}(bpy)_3]^{2+}$ (bpy =2.2′-bipyridine; E_{ox} = 1.24 V vs SCE), no electron transfer was observed. This is consistent with the lower one-electron reduction potential of **1** (E_{red} = 0.78 V vs SCE), as reported previously.[41b] The E_{red} value of **2** was also determined to be 0.80 V vs SCE by the redox titration using Br_2Fc (E_{ox} = 0.71 V vs SCE) (Figure 3b).

When the $Mn^{IV}(O)-(Sc^{3+})_1$ complex of **1** was employed with 2 equiv of $Sc(OTf)_3$ (2.0 mM), electron transfer from $[Ru^{II}(bpy)_3]^{2+}$ to the $Mn^{IV}(O)-(Sc^{3+})_1$ complex became energetically feasible to occur as shown in Figure 4a, where the absorption band (λ_{max} = 650 nm) due to $[Ru^{III}(bpy)_3]^{3+}$ increased. In this case, however, the electron transfer from $[Ru^{II}(bpy)_3]^{2+}$ to the $Mn^{IV}(O)-(Sc^{3+})_1$ complex was not complete with 2 equiv of $[Ru^{II}(bpy)_3]^{2+}$. Figure 4b shows the titration curve of the electron-transfer reaction, suggesting that electron transfer from $[Ru^{II}(bpy)_3]^{2+}$ to the $Mn^{IV}(O)-(Sc^{3+})_1$ complex is in equilibrium with back electron transfer from the $Mn^{III}(O)-(Sc^{3+})_1$ complex to $[Ru^{III}(bpy)_3]^{3+}$ (eq 1, where K_{et} is the electron-transfer equilibrium constant).

dx.doi.org/10.1021/ja403965h | J. Am. Chem. Soc. 2013, 135, 9186−9194

Table 1. One-Electron Oxidation Potentials (E_{ox}) of Electron Donors and Second-Order Rate Constants of Electron Transfer from Electron Donors to 1 and 2 in the Absence and Presence of $Sc(OTf)_3$ (10 mM) with Driving Force of Electron Transfer ($-\Delta G_{et}$) in CF_3CH_2OH/CH_3CN (v/v = 1:1) at 273 K

		$[(Bn\text{-}TPEN)Mn^{IV}(O)]^{2+}$ [a]		$[(N4Py)Mn^{IV}(O)]^{2+}$	
electron donor	E_{ox}, V vs SCE[a]	k_{obs}, M^{-1} s^{-1}	$-\Delta G_{et}$, eV	k_{obs}, M^{-1} s^{-1}	$-\Delta G_{et}$, eV
dimethylferrocene	0.26	$(1.0 \pm 0.1) \times 10^5$	0.52		
ferrocene	0.37	$(6.1 \pm 0.3) \times 10^3$	0.41	$(8.2 \pm 0.1) \times 10^3$	0.43
bromoferrocene	0.54	$(9.3 \pm 0.1) \times 10^2$	0.24	$(8.4 \pm 0.3) \times 10^2$	0.26
acetylferrocene	0.62	$(9.3 \pm 0.2) \times 10$	0.16	$(8.2 \pm 0.2) \times 10$	0.18
dibromoferrocene	0.71	$(3.1 \pm 0.1) \times 10$	0.07	$(4.3 \pm 0.1) \times 10$	0.09
		$[(Bn\text{-}TPEN)Mn^{IV}(O)]^{2+}\text{–}(Sc^{3+})_2$		$[(N4Py)Mn^{IV}(O)]^{2+}\text{–}(Sc^{3+})_2$	
electron donor	E_{ox}, V vs SCE[b]	k_{obs}, M^{-1} s^{-1}	$-\Delta G_{et}$, eV	k_{obs}, M^{-1} s^{-1}	$-\Delta G_{et}$, eV
$[Fe^{II}(Me_2\text{-}phen)_3]^{2+}$	0.94	$(1.7 \pm 0.2) \times 10^5$	0.42	$(2.3 \pm 0.1) \times 10^5$	0.48
$[Fe^{II}(Ph_2\text{-}phen)_3]^{2+}$	1.02	$(2.1 \pm 0.1) \times 10^4$	0.34	$(2.4 \pm 0.4) \times 10^4$	0.40
$[Fe^{II}(bpy)_3]^{2+}$	1.06	$(3.6 \pm 0.1) \times 10^3$	0.30	$(6.9 \pm 0.1) \times 10^3$	0.36
$[Fe^{II}(5\text{-}Cl\text{-}phen)_3]^{2+}$	1.20	$(4.1 \pm 0.8) \times 10^2$	0.16	$(4.1 \pm 0.2) \times 10^2$	0.22
$[Ru^{II}(bpy)_3]^{2+}$	1.24	$(7.3 \pm 0.1) \times 10$	0.12	$(6.4 \pm 0.3) \times 10$	0.18

[a]Taken from ref 41b. [b]Taken from ref 30b.

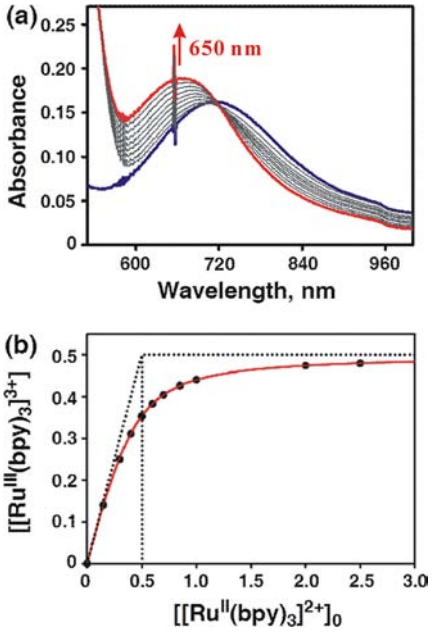

Figure 4. (a) Absorption spectral changes observed in electron transfer from $[Ru^{II}(bpy)]^{2+}$ (5.0×10^{-3} M) to $[(Bn\text{-}TPEN)Mn^{IV}(O)]^{2+}\text{–}Sc^{3+}$ (5.0×10^{-4} M) in CF_3CH_2OH/CH_3CN (v/v = 1:1) at 273 K. (b) Plot of concentration of $[Ru^{III}(bpy)_3]^{3+}$ produced in electron transfer from $[Ru^{II}(bpy)_3]^{2+}$ to $[(Bn\text{-}TPEN)Mn^{IV}(O)]^{2+}\text{–}Sc^{3+}$ vs initial concentration of $[Ru^{II}(bpy)_3]^{2+}$, $[[Ru^{II}(bpy)_3]^{2+}]_0$.

$$[Ru^{II}(bpy)_3]^{2+} + [Mn^{IV}(O)]^{2+}\text{–}Sc^{3+} \overset{K_{et}}{\rightleftharpoons} [Ru^{III}(bpy)_3]^{3+} + [Mn^{III}(O)]^{+}\text{–}Sc^{3+} \quad (1)$$

From the redox titration curve in Figure 4b, the K_{et} value was determined to be 5.7 (see a linear plot to determine the K_{et} value in Figure S4d in the SI).[43] The E_{red} value of 1.28 V vs SCE for $[(Bn\text{-}TPEN)Mn^{IV}(O)]^{2+}\text{–}(Sc^{3+})_1$ was determined from the K_{et} value and the E_{ox} value of $[Ru^{II}(bpy)_3]^{2+}$ (1.24 V vs SCE) using the Nernst equation (eq 2). This E_{red} value is significantly more positive than the E_{red} value of **1** (0.78 V vs SCE), which was reported previously.[41b]

$$E_{red} = E_{ox} + (RT/F) \ln K_{et} \quad (2)$$

Similarly, the E_{red} values of **1** and **2** in the presence of various concentrations of $Sc(OTf)_3$ were determined from the K_{et} values obtained by the redox titrations with $[Ru^{II}(bpy)_3]^{2+}$ (E_{ox} = 1.24 V vs SCE) and $[Ru^{II}(5\text{-}Cl\text{-}phen)_3]^{2+}$ (5-Cl-phen = 5-chloro-1,10-phenanthroline; E_{ox} = 1.36 V vs SCE; see Figures S4 and S5 in the SI). Figure 5 shows plots of E_{red} of **1** and **2** in the presence of various concentrations of $Sc(OTf)_3$. The E_{red} values of **1** and **2** were shifted from 0.78 and 0.80 V vs SCE in the absence of $Sc(OTf)_3$ to 1.28 and 1.31 V vs SCE in the presence of 1 equiv (for N4Py) or 2 equiv (for Bn-TPEN) of $Sc(OTf)_3$, which correspond to the E_{red} values of the $[Mn^{IV}(O)]^{2+}\text{–}Sc^{3+}$ complexes of **1** and **2**, respectively. The E_{red} values increase with increasing concentration of $Sc(OTf)_3$ to reach constant values with more than 6 equiv of $Sc(OTf)_3$. This is consistent with the UV–vis spectral change to produce the $[Mn^{IV}(O)]^{2+}\text{–}(Sc^{3+})_2$ complex in Figure 1b. The saturated E_{red} values of 1.36 and 1.42 V vs SCE in the presence of large excess $Sc(OTf)_3$ correspond to those of the $[Mn^{IV}(O)]^{2+}\text{–}(Sc^{3+})_2$ complexes of **1** and **2**, respectively. These E_{red} values are summarized in Table 2. There is a large difference in the E_{red} values between $[Mn^{IV}(O)]^{2+}$ and $[Mn^{IV}(O)]^{2+}\text{–}Sc^{3+}$, indicating that the binding of Sc^{3+} to $[Mn^{III}(O)]^{+}$ is much stronger than that to $[Mn^{IV}(O)]^{2+}$ as expected from the increased basicity of the oxo moiety in $[Mn^{III}(O)]^{+}$. The smaller difference in E_{red}

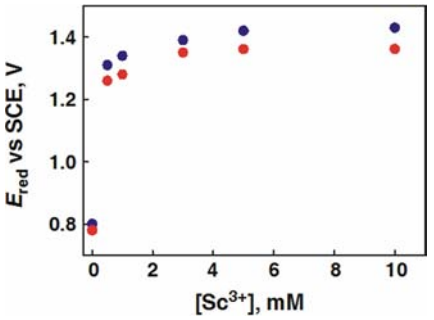

Figure 5. Dependence of E_{red} of $[(N4Py)Mn^{IV}(O)]^{2+}$ (blue circles) and $[(Bn\text{-}TPEN)Mn^{IV}(O)]^{2+}$ (red circles) on $[Sc^{3+}]$ in CF_3CH_2OH/CH_3CN (v/v = 1:1) at 273 K. The E_{red} values were determined from the equilibrium constants (K_{et}) between one electron donors and $[(N4Py)Mn^{IV}(O)]^{2+}$.

dx.doi.org/10.1021/ja403965h | J. Am. Chem. Soc. 2013, 135, 9186–9194

Table 2. One-Electron Reduction Potentials (E_{red}) and Reorganization Energies (λ) of Electron-Transfer Reduction of $[Mn^{IV}(O)]^{2+}$, $[Mn^{IV}(O)]^{2+}-(Sc^{3+})_1$, and $[Mn^{IV}(O)]^{2+}-(Sc^{3+})_2$

complex	E_{red}, V vs SCE	λ, eV
$[(Bn\text{-}TPEN)Mn^{IV}(O)]^{2+}$	0.78 ± 0.01[a]	2.24 ± 0.03[a]
$[(Bn\text{-}TPEN)Mn^{IV}(O)]^{2+}-(Sc^{3+})_1$	1.28 ± 0.02	
$[(Bn\text{-}TPEN)Mn^{IV}(O)]^{2+}-(Sc^{3+})_2$	1.36 ± 0.02	2.12 ± 0.02
$[(N4Py)Mn^{IV}(O)]^{2+}$	0.80 ± 0.01	2.27 ± 0.03
$[(N4Py)Mn^{IV}(O)]^{2+}-(Sc^{3+})_1$	1.31 ± 0.02	
$[(N4Py)Mn^{IV}(O)]^{2+}-(Sc^{3+})_2$	1.42 ± 0.01	2.21 ± 0.02

[a]Taken from ref 41b.

between $[Mn^{IV}(O)^{2+}]-(Sc^{3+})_1$ and $[Mn^{IV}(O)]^{2+}-(Sc^{3+})_2$ may support the previous conclusion based on XANES/EXAFS analysis together with DFT calculations: second Sc^{3+} ion is located at the secondary coordination sphere rather than direct binding to the oxo moiety.[37]

Comparison of Electron-Transfer Reactivity of Non-heme $Mn^{IV}(O)$ Complexes with and without Sc^{3+} Ions. A remarkable positive shift of E_{red} values of $[Mn^{IV}(O)]^{2+}$ complexes by binding one or two Sc^{3+} ions predicts the much enhanced electron-transfer reactivity. Rate constants of electron transfer from various electron donors to **1** and **2** in the absence and presence of Sc^{3+} were determined by monitoring the absorbance changes in reaction solutions due to the oxidized electron donors. Rates of electron transfer in the absence of Sc^{3+} obeyed pseudo-first-order kinetics in the presence of large excess of electron donors, and the observed pseudo-first-order rate constants (k_{obs}) increased linearly with no intercept with concentrations of electron donors (Figure S6 in the SI). Rate constants of electron transfer from one-electron reductants to **1** and **2** in the presence of Sc^{3+} were determined under second-order reaction conditions (Figures S7 and S8 in the SI). The k_{et} values increased with increasing concentration of Sc^{3+} in the conversion of $[Mn^{IV}(O)]^{2+}$ to $[Mn^{IV}(O)]^{2+}-(Sc^{3+})_2$ (Figure 6). The k_{et} values thus determined are listed in Table 1 along with the one-electron oxidation potentials (E_{ox}) of donors and the driving force of electron transfer ($-\Delta G_{et}$).

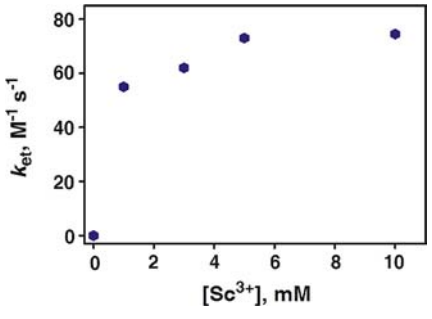

Figure 6. Dependence of k_{et} on $[Sc^{3+}]$ for electron transfer from $[Ru^{II}(bpy)_3]^{2+}$ to $[(Bn\text{-}TPEN)Mn^{IV}(O)]^{2+}$ in CF_3CH_2OH/CH_3CN (v/v = 1:1) at 273 K.

Figure 7 shows comparison of dependence of k_{et} on E_{ox} of electron donors for electron transfer from electron donors to $[(Bn\text{-}TPEN)Mn^{IV}(O)]^{2+}$ (**1**) with that of electron transfer to $[(Bn\text{-}TPEN)Mn^{IV}(O)]^{2+}-(Sc^{3+})_2$ in the absence and presence of $Sc(OTf)_3$ (5.0 mM) in CF_3CH_2OH/CH_3CN (v/v = 1:1) at 273 K. The k_{et} values of $[Mn^{IV}(O)]^{2+}-(Sc^{3+})_2$ are much larger than those of $[Mn^{IV}(O)]^{2+}$.

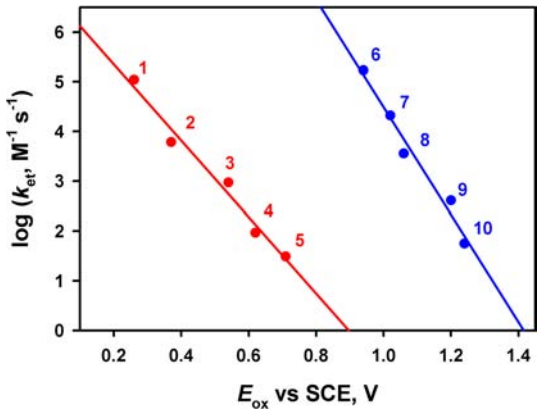

Figure 7. Plots of log k_{et} vs the one-electron oxidation potentials of electron donors (E_{ox}) for electron transfer from various electron donors [(1) dimethylferrocene, (2) ferrocene, (3) bromoferrocene, (4) acetylferrocene, (5) Br_2Fc, (6) $[Fe^{II}(Me_2\text{-}phen)_3]^{2+}$, (7) $[Fe^{II}(Ph_2\text{-}phen)_3]^{2+}$, (8) $[Fe^{II}(bpy)_3]^{2+}$, (9) $[Fe^{II}(5\text{-}Cl\text{-}phen)_3]^{2+}$, and (10) $[Ru^{II}(bpy)_3]^{2+}$] to $[(Bn\text{-}TPEN)Mn^{IV}(O)]^{2+}$ (red line) and $[(Mn^{IV}(O)]^{2+}-(Sc^{3+})_2$ (blue line) in CF_3CH_2OH/CH_3CN (v/v = 1:1) at 273 K.

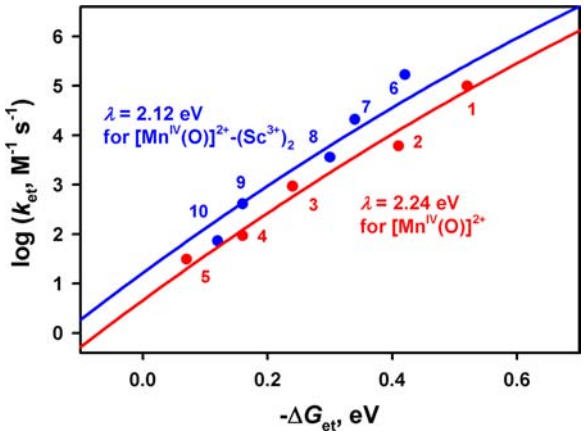

Figure 8. Driving force ($-\Delta G_{et}$) dependence of rate constants (log k_{et}) of electron transfer from one-electron donors [(1) dimethylferrocene, (2) ferrocene, (3) bromoferrocene, (4) acetylferrocene, (5) Br_2Fc, (6) $[Fe^{II}(Me_2\text{-}phen)_3]^{2+}$, (7) $[Fe^{II}(Ph_2\text{-}phen)_3]^{2+}$, (8) $[Fe^{II}(bpy)_3]^{2+}$, (9) $[Fe^{II}(5\text{-}Cl\text{-}phen)_3]^{2+}$, and (10) $[Ru^{II}(bpy)_3]^{2+}$] to $[(Bn\text{-}TPEN)Mn^{IV}(O)]^{2+}$ (red circles) and $[(Bn\text{-}TPEN)Mn^{IV}(O)]^{2+}-(Sc^{3+})_2$ (blue circles) in CF_3CH_2OH/CH_3CN (v/v = 1:1) at 273 K. The blue and red lines are the Marcus lines calculated with λ values of 2.12 and 2.24 eV, respectively.

The driving force dependences of the rate constants of electron transfer from electron donors to $[Mn^{IV}(O)]^{2+}$ and $[Mn^{IV}(O)]^{2+}-(Sc^{3+})_2$ for **1** are shown in Figure 8, where two different plots in Figure 7 are largely unified. The driving force dependence of log k_{et} is well fitted by the solid line in Figure 8 in light of the Marcus theory of adiabatic outer-sphere electron transfer (eq 3)[47]

$$k_{et} = Z \exp[-(\lambda/4)(1 + \Delta G_{et}/\lambda)^2/k_B T] \quad (3)$$

where Z is the collision frequency taken as 1×10^{11} M^{-1} s^{-1}, λ is the reorganization energy of electron transfer, k_B is the Boltzmann constant, and T is the absolute temperature. The closer look of the fitting afforded slightly different λ values, such as one for $[(Bn\text{-}TPEN)Mn^{IV}(O)]^{2+}$ (2.24 ± 0.03 eV) and the other for $[(Bn\text{-}TPEN)Mn^{IV}(O)]^{2+}-(Sc^{3+})_2$ (2.12 ± 0.02 eV).

dx.doi.org/10.1021/ja403965h | J. Am. Chem. Soc. 2013, 135, 9186−9194

Similarly, the other λ values were determined with the E_{red} values, as listed in Table 2.

The λ values of the electron-transfer reduction of $[Mn^{IV}(O)]^{2+}$ are similar to those determined for the electron-transfer reduction of iron(IV)−oxo complexes.[23b] This indicates that the one-electron reduction of high-valent metal−oxo complexes generally requires a large reorganization energy probably due to the significant elongation of metal−oxo bond upon one-electron reduction. The smaller λ value of $[Mn^{IV}(O)]^{2+}$−$(Sc^{3+})_2$, as compared with $[Mn^{IV}(O)]^{2+}$, may be explained by the elongation of the Mn^{IV}−O bond prior to electron transfer because of binding of two Sc^{3+} ions, which results in smaller change in the Mn−O bond distance upon the electron transfer. It should be noted that $[(N4Py)Mn^{IV}(O)]^{2+}$−$(Sc^{3+})_2$ has the most positive E_{red} value as compared with those of iron(IV)−oxo complexes.[23] Thus, $[(N4Py)Mn^{IV}(O)]^{2+}$−$(Sc^{3+})_2$ is regarded as the strongest oxidant among high-valent metal−oxo complexes reported so far.

Change in Mechanism from Direct Oxygen Atom Transfer to Electron Transfer in Sulfoxidation of Thioanisoles with Nonheme $Mn^{IV}(O)$ Complexes by Binding of Sc^{3+} Ions. We have suggested previously that the mechanism of sulfoxidation of thioanisoles with $[(N4Py)Mn^{IV}(O)]^{2+}$ is changed from direct oxygen atom transfer (DOT) to electron transfer (ET) when Sc^{3+} ions are bound to $[(N4Py)Mn^{IV}(O)]^{2+}$.[37] This proposal is now verified by the electron-transfer driving force dependence of log k_{obs} for sulfoxidation of thioanisoles with $[(N4Py)Mn^{IV}(O)]^{2+}$ vs $[(N4Py)Mn^{IV}(O)]^{2+}$−$(Sc^{3+})_2$ (Figure 9). The k_{obs} values of sulfoxidation of thioanisoles with $[(N4Py)Mn^{IV}(O)]^{2+}$ are much larger than the predicted values of the solid line drawn

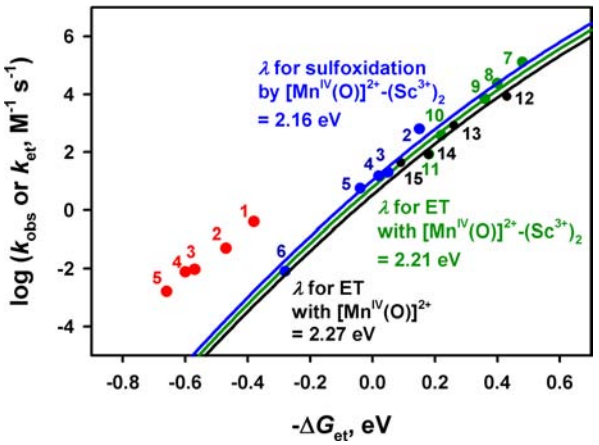

Figure 9. Plots of log k_{obs} for sulfoxidation of *para*-X-substituted thioanisoles [X = (1) MeO, (2) Me, (3) H, (4) F, (5) Br, and (6) CN] with $[(N4Py)Mn^{IV}(O)]^{2+}$ (0.50 mM) in CF_3CH_2OH/CH_3CN (v/v = 19:1) at 273 K vs the driving force of electron transfer [$-\Delta G_{et} = e(E_{red} - E_{ox})$] from the thioanisoles to $[(N4Py)Mn^{IV}(O)]^{2+}$ in the absence of Sc^{3+} (red circles) and the presence of 5.0 mM Sc^{3+} (blue circles). The k_{obs} values for the sulfoxidation were taken from ref 37. The black and green circles show the driving-force dependence of the rate constants (log k_{et}) for electron transfer from one-electron reductants [(7) $[Fe^{II}(Me_2\text{-phen})_3]^{2+}$, (8) $[Fe^{II}(Ph_2\text{-phen})_3]^{2+}$, (9) $[Fe^{II}(bpy)_3]^{2+}$, (10) $[Fe^{II}(5\text{-Cl-phen})_3]^{2+}$, (11) $[Ru^{II}(bpy)_3]^{2+}$, (12) ferrocene, (13) bromoferrocene, (14) acetylferrocene, and (15) Br_2Fc] to $[(N4Py)Mn^{IV}(O)]^{2+}$ in the absence of Sc^{3+} (black circles) and the presence of 5.0 mM Sc^{3+} (green circles) in CF_3CH_2OH/CH_3CN (v/v = 1:1) at 273 K. The blue, green, and black lines are the best fit of the Marcus lines calculated for blue, green, and black circles, respectively.

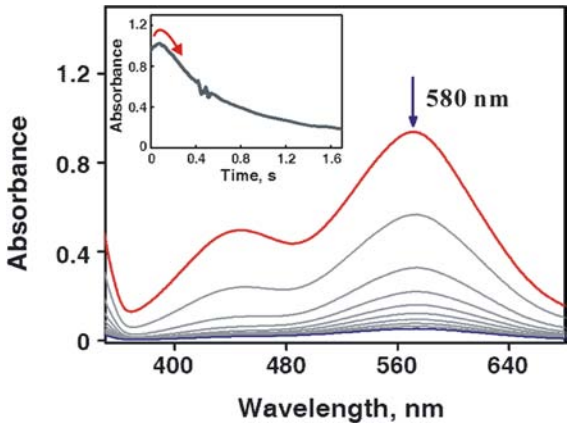

Figure 10. UV−vis spectral changes in the reaction of $[(N4Py)Mn^{IV}(O)]^{2+}$ (6.25×10^{-5} M) with *p*-methoxythioanisole (1.25×10^{-3} M) in the presence of $Sc(OTf)_3$ (6.25×10^{-4} M) in CF_3CH_2OH/CH_3CN (v/v = 1:1) at 273 K. Inset shows the time course of absorbance at 580 nm due to *p*-methoxythioanisole radical cation.

Scheme 1

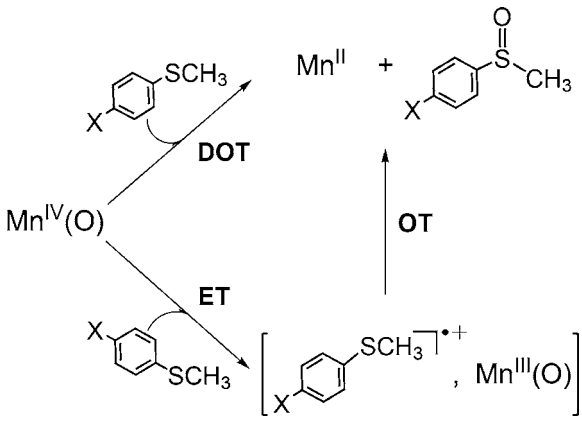

based on eq 3 for outer-sphere electron-transfer reactions. This implies that much stronger interaction between thioanisoles and $[(N4Py)Mn^{IV}(O)]^{2+}$ is required in the sulfoxidation reaction as compared with outer-sphere electron transfer from thioanisoles to $[(N4Py)Mn^{IV}(O)]^{2+}$. Thus, the sulfoxidation reaction with $[(N4Py)Mn^{IV}(O)]^{2+}$ proceeds via direct oxygen atom transfer. In contrast, the rate constants of sulfoxidation of thioanisoles with $[(N4Py)Mn^{IV}(O)]^{2+}$−$(Sc^{3+})_2$ fit well in the Marcus line for electron transfer from one-electron reductants to $[(N4Py)Mn^{IV}(O)]^{2+}$−$(Sc^{3+})_2$. Such an agreement clearly indicates that the sulfoxidation of thioanisoles by $[(N4Py)Mn^{IV}(O)]^{2+}$−$(Sc^{3+})_2$ proceeds via an outer-sphere electron-transfer pathway (Figure 9).

The occurrence of electron transfer was confirmed in the case of *p*-methoxythioanisole in the presence of $Sc(OTf)_3$ (5.0 mM), where the driving force for electron transfer is positive ($-\Delta G_{et}$ = 0.20 eV; i.e., a thermodynamically favorable process). As shown in Figure 10, the transient absorption band at 580 nm due to *p*-methoxythioanisole radical cation appeared instantly, followed by a relatively slow decay (see ref 30b for the reference spectrum of *p*-methoxythioanisole radical cation). The absorption band at 635 nm due to $[(N4Py)Mn^{IV}(O)]^{2+}$−$(Sc^{3+})_2$ was not detected even with a stopped-flow spectrometer since electron transfer from *p*-methoxythioanisole to $[(N4Py)Mn^{IV}(O)]^{2+}$−$(Sc^{3+})_2$[37] was extremely fast. These

dx.doi.org/10.1021/ja403965h | J. Am. Chem. Soc. 2013, 135, 9186−9194

results clearly demonstrate that the electron-transfer pathway (ET/OT in Scheme 1) becomes dominant over the oxygen atom transfer pathway (DOT in Scheme 1) when the sulfoxidation by the $Mn^{IV}(O)$ complex is carried out in the presence of Sc^{3+}.

CONCLUSION

The electron-transfer reactivity of nonheme $Mn^{IV}(O)$ complexes was enhanced as much as 10^7−fold by binding of Sc^{3+} ions. A large positive shift in the one-electron reduction potential was observed by binding of Sc^{3+} ions to $[Mn^{IV}(O)]^{2+}$ (e.g., from 0.80 V of $[(N4Py)Mn^{IV}(O)]^{2+}$ to 1.42 V of $[(N4Py)Mn^{IV}(O)]^{2+}$−$(Sc^{3+})_2$). The reorganization energy of electron transfer becomes smaller by binding of Sc^{3+} ions because of the elongation of Mn^{IV}−O bond, which results in a smaller change in the Mn−O distance upon the electron transfer. Thus, nonheme $Mn^{IV}(O)$ complexes become much stronger oxidants by binding of Sc^{3+} ions, resulting in the change of mechanism in the sulfoxidation of thioanisoles by $Mn^{IV}(O)$ complexes, such as from a direct oxygen atom transfer pathway by $[Mn^{IV}(O)]^{2+}$ to an electron transfer pathway by $[Mn^{IV}(O)]^{2+}$−$(Sc^{3+})_x$. The remarkable enhancement of the electron-transfer reactivity of $Mn^{IV}(O)$ complexes by binding of Sc^{3+} ions may pave a new way to improve the catalytic reactivity of metal−oxo complexes in oxidation reactions.

EXPERIMENTAL SECTION

Materials. Commercially available chemicals were used without further purification unless otherwise indicated. Solvents were dried according to published procedures and distilled under Ar prior to use.[48] Scandium triflate, $Sc(OTf)_3$ (OTf = $SO_3CF_3^-$), was purchased from Aldrich and used as received. Iodosylbenzene (PhIO) was prepared by a literature method.[49] N4Py and Bn-TPEN ligands and $Mn^{II}(OTf)_2{\cdot}2CH_3CN$ were prepared by literature methods.[20b,50] The $[(N4Py)Mn^{II}(CH_3CN)](CF_3SO_3)_2$ and $[(Bn\text{-}TPEN)\text{-}Mn^{II}(CH_3CN)](CF_3SO_3)_2$ complexes were prepared in a drybox.[37,41] N4Py (0.54 mmol, 0.20 g) and $Mn^{II}(OTf)_2{\cdot}2CH_3CN$ (0.82 mmol, 0.32 g) were dissolved in CH_3CN, and the reaction solution was stirred at ambient temperature overnight. The resulting solution was filtered and added to a large volume of Et_2O. The product was obtained as a white solid with 60% yield (0.24 g). Bn-TPEN (0.47 mmol, 0.20 g) and $Mn^{II}(CF_3SO_3)_2{\cdot}2CH_3CN$ (0.57 mmol, 0.25 g) were dissolved in CH_3CN and stirred at ambient temperature overnight. The resulting solution was filtered and added to a large volume of Et_2O. The product was obtained as a white solid in 85% yield (0.38 g). One-electron reductants, such as $[Fe^{II}(Me_2\text{-phen})_3]^{2+}$, $[Fe^{II}(Ph_2\text{-phen})_3]^{2+}$, $[Fe^{II}(bpy)_3]^{2+}$, $[Fe^{II}(5\text{-Cl-phen})_3]^{2+}$, and $[Ru^{II}(bpy)_3]^{2+}$, were synthesized according to literature methods.[51]

DFT Calculations. Calculations were done with density functional theory (DFT)[44] using the Gaussian 09 package[52] and the B3LYP functional.[53] Optimizing and single-point frequency calculations were done with the LACVP basis set[54] (except for S, which required 6-311+G*), while a single-point evaluation was done using the LACV3P*+ basis set[54] in order to obtain more accurate Mulliken spin density distribution. All calculations (including the optimizations) were done in solvent (acetonitrile) using the CPCM scheme.[55]

Redox Titrations. Electron transfer from dibromoferrocene to $[Mn^{IV}(O)]^{2+}$ (5.0×10^{-4} M) was examined from the spectral change in the various concentration of dibromoferrocene (1.5×10^{-4} to 5.0×10^{-2} M) at 273 K. Typically, a deaerated CH_3CN solution of dibromoferrocene (7.5×10^{-5} − 5.0×10^{-4} M) was added to a deaerated trifluoroethanol solution containing $[Mn^{IV}(O)]^{2+}$ (5.0×10^{-4} M). The concentration of dibromoferrocenium ion (Br_2Fc^+) was determined from the absorption band at λ = 700 nm due to Br_2Fc^+ ($\varepsilon = 4.0 \times 10^2$ M^{-1} cm^{-1}). The ε value of Br_2Fc^+ was determined by the electron-transfer oxidation of Br_2Fc with cerium(IV) ammonium nitrate (5.0×10^{-3} M) in CF_3CH_2OH/MeCN (v/v = 1:1) at 273 K. Likewise, electron transfer from $[Ru^{II}(bpy)_3]^{2+}$ to $[Mn^{IV}(O)]^{2+}$−$(Sc^{3+})_1$ (5.0×10^{-4} M) and $[Ru^{II}(5\text{-Cl-phen})_3]^{2+}$ to $[Mn^{IV}(O)]^{2+}$−$(Sc^{3+})_2$ (5.0×10^{-4} M) were examined from the spectral change in the various concentration of $[Ru^{II}(bpy)_3]^{2+}$ (1.5×10^{-4} to 5.0×10^{-2} M) and $[Ru^{II}(5\text{-Cl-phen})_3]^{2+}$ at 273 K.

Kinetic Measurements. Kinetic measurements were performed in CF_3CH_2OH/CH_3CN (v/v = 1:1) at 273 K. Rates of electron transfer from ferrocene derivatives to $[Mn^{IV}(O)]^{2+}$ (2.5×10^{-4} M) were investigated by the formation and decay of absorption bands due to ferrocenium ion and $[Mn^{IV}(O)]^{2+}$, respectively. Kinetic measurements for rates of electron transfer from various electron donors to $[Mn^{IV}(O)]^{2+}$−$(Sc^{3+})_1$ and $[Mn^{IV}(O)]^{2+}$−$(Sc^{3+})_2$ were carried out under second-order conditions, where both concentrations of electron donors and $[Mn^{IV}(O)]^{2+}$−$(Sc^{3+})_1$ or $[Mn^{IV}(O)]^{2+}$−$(Sc^{3+})_2$ were 1.25×10^{-4} M, because electron transfer rates were too fast to follow under pseudo-order conditions even with use of a stopped-flow equipment.

Instrumentation. UV−vis spectra were recorded on a Hewlett-Packard 8453 diode array spectrophotometer equipped with a UNISOKU Scientific Instruments Cryostat USP-203A for low-temperature experiments or on a UNISOKU RSP-601 stopped-flow spectrometer equipped with a MOS-type highly sensitive photodiode-array. X-band EPR spectra were recorded at 5 K using X-band Bruker EMX-plus spectrometer equipped with a dual mode cavity (ER 4116DM). Low temperature was achieved and controlled with an Oxford Instruments ESR900 liquid He quartz cryostat with an Oxford Instruments ITC503 temperature and gas flow controller. The experimental parameters for EPR measurement were as follows: microwave frequency = 9.646 GHz, microwave power = 1.0 mW, modulation amplitude = 10 G, gain = 1.0×10^4, modulation frequency = 100 kHz, time constant = 40.96 ms, and conversion time = 81.00 ms.

ASSOCIATED CONTENT

Supporting Information

Experimental section for X-ray absorption spectroscopy (XAS), EXAFS least-squares fitting results (Table S1), DFT calculation (Tables S2 and S3), EPR spectra (Figure S1), XAS spectra (Figure S2), first and second binding constants (Figure S3), redox titrations (Figures S4 and S5), kinetic data (Figures S6−S8), DFT calculated coordinates, and complete ref 52. This material is available free of charge via the Internet at http://pubs.acs.org.

AUTHOR INFORMATION

Corresponding Author

fukuzumi@chem.eng.osaka-u.ac.jp; wwnam@ewha.ac.kr

Notes

The authors declare no competing financial interest.

ACKNOWLEDGMENTS

The research at OU was supported by Grant-in-Aid (No. 20108010 to S.F.) and Global COE program, "the Global Education and Research Center for Bio-Environmental Chemistry" from the Ministry of Education, Culture, Sports, Science and Technology, Japan (to S.F.). The research at EWU was supported by NRF/MEST of Korea through CRI (to W.N.), GRL (2010-00353) (to W.N.), 2011 KRICT OASIS project (to W.N.), and WCU (R31-2008-000-10010-0) (to W.N. and S.F.). XAS data were measured at the Stanford Synchrotron Radiation Lightsource (SSRL), a Directorate of SLAC National Accelerator Laboratory, and an Office of Science User Facility operated for the U.S. Department of Energy Office of Science by Stanford University. The SSRL Structural Molecular Biology Program is supported by the National Institutes of Health and by the Department of Energy,

Office of Biological and Environmental Research (BER). The publication was partially supported by National Institutes of Health (NIH) Grant No. 5 P41 RR001209.

REFERENCES

(1) (a) Ortiz de Montellano, P. R. *Cytochrome P450: Structure, Mechanism, and Biochemistry*, 3rd ed.; Kluwer Academic/Plenum Publishers: New York, 2005. (b) Meunier, B., Ed. *Biomimetic Oxidations Catalyzed by Transition Metal Complexes*; Imperial College Press: London, 2000. (c) *The Ubiquitous Role of Cytochrome P450 Proteins In Metal Ions in Life Sciences*; Sigel, A., Sigel, H., Sigel, R. K. O., Eds.; John Wiley & Sons Ltd.: Chichester, England, 2007; Vol. 3.

(2) (a) Sono, M.; Roach, M. P.; Coulter, E. D.; Dawson, J. H. *Chem. Rev.* **1996**, *96*, 2841. (b) Watanabe, Y. *J. Biol. Inorg. Chem.* **2001**, *6*, 846. (c) Jung, C. *Biochim. Biophys. Acta* **2011**, *1814*, 46. (d) Denisov, I. G.; Makris, T. M.; Sligar, S. G.; Schlichting, I. *Chem. Rev.* **2005**, *105*, 2253.

(3) (a) Rittle, J.; Green, M. T. *Science* **2010**, *330*, 933. (b) Makris, T. M.; von Koenig, K.; Schlichting, I.; Sligar, S. G. *J. Inorg. Biochem.* **2006**, *100*, 507. (c) Groves, J. T. *Proc. Natl. Acad. Sci. U.S.A.* **2003**, *100*, 3569. (d) Groves, J. T. *J. Inorg. Biochem.* **2006**, *100*, 434.

(4) (a) Usharani, D.; Janardanan, D.; Li, C.; Shaik, S. *Acc. Chem. Res.* **2013**, *46*, 471. (b) Krebs, C.; Fujimori, D. G.; Walsh, C. T.; Bollinger, J. M., Jr. *Acc. Chem. Res.* **2007**, *40*, 484.

(5) (a) Proshlyakov, D. A.; Henshaw, T. F.; Monterosso, G. R.; Ryle, M. J.; Hausinger, R. P. *J. Am. Chem. Soc.* **2004**, *126*, 1022. (b) Price, J. C.; Barr, E. W.; Hoffart, L. M.; Krebs, C.; Bollinger, J. M., Jr. *Biochemistry* **2005**, *44*, 8138. (c) Price, J. C.; Barr, E. W.; Glass, T. E.; Krebs, C.; Bollinger, J. M., Jr. *J. Am. Chem. Soc.* **2003**, *125*, 13008.

(6) (a) Tinberg, C. E.; Lippard, S. J. *Acc. Chem. Res.* **2011**, *44*, 280. (b) Siewert, I.; Limberg, C. *Chem.—Eur. J.* **2009**, *15*, 10316.

(7) (a) Hammarström, L.; Hammes-Schiffer, S. *Acc. Chem. Res.* **2009**, *42*, 1859. (b) McEvoy, J. P.; Brudvig, G. W. *Chem. Rev.* **2006**, *106*, 4455. (c) Pecoraro, V. L.; Hsieh, W.-Y. *Inorg. Chem.* **2008**, *47*, 1765.

(8) (a) Umena, Y.; Kawakami, K.; Shen, J.-R.; Kamiya, N. *Nature* **2011**, *473*, 55. (b) Siegbahn, P. E. M. *Acc. Chem. Res.* **2009**, *42*, 1871.

(9) (a) Borovik, A. S. *Acc. Chem. Res.* **2005**, *38*, 54. (b) Benet-Buchholz, J.; Comba, P.; Llobet, A.; Roeser, S.; Vadivelu, P.; Wadepohl, W.; Wiesner, S. *Dalton Trans.* **2009**, 5910. (c) Hohenberger, J.; Ray, K.; Meyer, K. *Nat. Commun.* **2012**, *3*, 720.

(10) (a) de Visser, S. P.; Rohde, J.-U.; Lee, Y.-M.; Cho, J.; Nam, W. *Coord. Chem. Rev.* **2013**, *257*, 381. (b) McDonald, A. R.; Que, L., Jr. *Coord. Chem. Rev.* **2013**, *257*, 414.

(11) (a) Meunier, B.; de Visser, S. P.; Shaik, S. *Chem. Rev.* **2004**, *104*, 3947. (b) Shaik, S.; Cohen, S.; Wang, Y.; Chen, H.; Kumar, D.; Thiel, W. *Chem. Rev.* **2010**, *110*, 949. (c) Abu-Omar, M. M.; Loaiza, A.; Hontzeas, N. *Chem. Rev.* **2005**, *105*, 2227. (d) Denisov, I. G.; Makris, T. M.; Sligar, S. G.; Schlichting, I. *Chem. Rev.* **2005**, *105*, 2253. (e) Ortiz de Montellano, P. R. *Chem. Rev.* **2010**, *110*, 932.

(12) (a) Gunay, A.; Theopold, K. H. *Chem. Rev.* **2010**, *110*, 1060. (b) Costas, M. *Coord. Chem. Rev.* **2011**, *255*, 2912.

(13) (a) Yin, G. *Acc. Chem. Res.* **2013**, *46*, 483. (b) Yin, G. *Coord. Chem. Rev.* **2010**, *254*, 1826.

(14) (a) Liua, H.-Y.; HR Mahmooda, M.; Qiuc, S.-X.; Chang, C. K. *Coord. Chem. Rev.* **2013**, *257*, 1306. (b) Goldberg, D. P. *Acc. Chem. Res.* **2007**, *40*, 626.

(15) (a) Cho, J.; Sarangi, R.; Nam, W. *Acc. Chem. Res.* **2012**, *45*, 1321. (b) Cho, J.; Woo, J.; Han, J. E.; Kubo, M.; Ogura, T.; Nam, W. *Chem. Sci.* **2011**, *2*, 2057.

(16) (a) Cho, J.; Jeon, S.; Wilson, S. A.; Liu, L. V.; Kang, E. A.; Braymer, J. J.; Lim, M. H.; Hedman, B.; Hodgson, K. O.; Valentine, J. S.; Solomon, E. I.; Nam, W. *Nature* **2011**, *478*, 502. (b) Rohde, J.-U.; In, J.-H.; Lim, M. H.; Brennessel, W. W.; Bukowski, M. R.; Stubna, A.; Münck, E.; Nam, W.; Que, L., Jr. *Science* **2003**, *299*, 1037.

(17) (a) Nam, W. *Acc. Chem. Res.* **2007**, *40*, 522. (b) Que, L., Jr. *Acc. Chem. Res.* **2007**, *40*, 493.

(18) (a) Gross, Z. *J. Biol. Inorg. Chem.* **2001**, *6*, 733. (b) Kerber, W. D.; Goldberg, D. P. *J. Inorg. Biochem.* **2006**, *100*, 838.

(19) (a) Mayer, J. M. *Acc. Chem. Res.* **2011**, *44*, 36. (b) Che, C.-M.; Lo, V. K.-Y.; Zhou, C.-Y.; Huang, J.-S. *Chem. Soc. Rev.* **2011**, *40*, 1950.

(20) (a) Lubben, M.; Meetsma, A.; Wilkinson, E. C.; Feringa, B.; Que, L., Jr. *Angew. Chem., Int. Ed.* **1995**, *34*, 1512. (b) Kaizer, J.; Klinker, E. J.; Oh, N. Y.; Rohde, J.-U.; Song, W. J.; Stubna, A.; Kim, J.; Münck, E.; Nam, W.; Que, L., Jr. *J. Am. Chem. Soc.* **2004**, *126*, 472. (c) Klinker, E. J.; Kaizer, J.; Brennessel, W. W.; Woodrum, N. L.; Cramer, C. J.; Que, L., Jr. *Angew. Chem., Int. Ed.* **2005**, *44*, 3690.

(21) (a) Hong, S.; Lee, Y.-M.; Cho, K.-B.; Sundaravel, K.; Cho, J.; Kim, M. J.; Shin, W.; Nam, W. *J. Am. Chem. Soc.* **2011**, *133*, 11876. (b) Tang, H.; Guan, J.; Zhang, L.; Liu, H.; Huang, X. *Phys. Chem. Chem. Phys.* **2012**, *14*, 12863. (c) Kumar, D.; Sastry, G. N.; de Visser, S. P. *J. Phys. Chem. B* **2012**, *116*, 718.

(22) (a) Arias, J.; Newlands, C. R.; Abu-Omar, M. M. *Inorg. Chem.* **2001**, *40*, 2185. (b) Prokop, K. A.; Neu, H. M.; de Visser, S. P.; Goldberg, D. P. *J. Am. Chem. Soc.* **2011**, *133*, 15874. (c) Fertinger, C.; Hessenauer-Ilicheva, N.; Franke, A.; van Eldik, R. *Chem.—Eur. J.* **2009**, *15*, 13435. (d) Arunkumar, C.; Lee, Y.-M.; Lee, J. Y.; Fukuzumi, S.; Nam, W. *Chem.—Eur. J.* **2009**, *15*, 11482. (e) Kumar, A.; Goldberg, I.; Botoshansky, M.; Buchman, Y.; Gross, Z. *J. Am. Chem. Soc.* **2010**, *132*, 15233. (f) Benet-Buchholz, J.; Comba, P.; Llobet, A.; Roeser, S.; Vadivelu, P.; Wiesner, S. *Dalton Trans.* **2010**, *39*, 3315.

(23) (a) Fukuzumi, S. *Coord. Chem. Rev.* **2013**, *257*, 1564. (b) Lee, Y.-M.; Kotani, H.; Suenobu, T.; Nam, W.; Fukuzumi, S. *J. Am. Chem. Soc.* **2008**, *130*, 434. (c) Fukuzumi, S.; Kotani, H.; Suenobu, T.; Hong, S.; Lee, Y.-M.; Nam, W. *Chem.—Eur. J.* **2010**, *16*, 354. (d) Comba, P.; Fukuzumi, S.; Kotani, H.; Wunderlich, S. *Angew. Chem., Int. Ed.* **2010**, *49*, 2622.

(24) Fukuzumi, S.; Kotani, H.; Prokop, K. A.; Goldberg, D. P. *J. Am. Chem. Soc.* **2011**, *133*, 1859.

(25) (a) Park, M. J.; Lee, J.; Suh, Y.; Kim, J.; Nam, W. *J. Am. Chem. Soc.* **2006**, *128*, 2630. (b) Sastri, C. V.; Lee, J.; Oh, K.; Lee, Y. J.; Lee, J.; Jackson, T. A.; Ray, K.; Hirao, H.; Shin, W.; Halfen, J. A.; Kim, J.; Que, L., Jr.; Shaik, S.; Nam, W. *Proc. Natl. Acad. Sci. U.S.A.* **2007**, *104*, 19181. (c) Jeong, Y. J.; Kang, Y.; Han, A.-R.; Lee, Y.-M.; Kotani, H.; Fukuzumi, S.; Nam, W. *Angew. Chem., Int. Ed.* **2008**, *47*, 7321. (d) Lee, Y.-M.; Dhuri, S. N.; Sawant, S. C.; Cho, J.; Kubo, M.; Ogura, T.; Fukuzumi, S.; Nam, W. *Angew. Chem., Int. Ed.* **2009**, *48*, 1803.

(26) (a) Lee, Y.-M.; Hong, S.; Morimoto, Y.; Shin, W.; Fukuzumi, S.; Nam, W. *J. Am. Chem. Soc.* **2010**, *132*, 10668. (b) Wilson, S. A.; Chen, J.; Hong, S.; Lee, Y.-M.; Clémancey, M.; Garcia-Serres, R.; Nomura, T.; Ogura, T.; Latour, J.-M.; Hedman, B.; Hodfson, K. O.; Nam, W.; Solomon, E. I. *J. Am. Chem. Soc.* **2012**, *134*, 11791.

(27) (a) England, J.; Guo, Y.; Van Heuvelen, K. M.; Cranswick, M. A.; Rohde, G. T.; Bominaar, E. L.; Münck, E.; Que, L., Jr. *J. Am. Chem. Soc.* **2011**, *133*, 11880. (b) Xue, G.; De Hont, R.; Münck, E.; Que, L., Jr. *Nat. Chem.* **2010**, *2*, 400. (c) Xue, G.; Fiedler, A. T.; Martinho, M.; Münck, E.; Que, L., Jr. *Proc. Natl. Acad. Sci. U.S.A.* **2008**, *105*, 20615. (d) Shanmugam, M.; Xue, G.; Que, L., Jr.; Hoffman, B. M. *Inorg. Chem.* **2012**, *51*, 10080.

(28) (a) Gupta, R.; A. S. Borovik, A. S. *J. Am. Chem. Soc.* **2003**, *125*, 13234. (b) Pestovsky, O.; Bakac, A. *J. Am. Chem. Soc.* **2004**, *126*, 13757. (c) Lam, W. W. Y.; Man, W.-L.; Lau, T,-C. *Coord. Chem. Rev.* **2007**, *251*, 2238. (d) de Visser, S. P. *J. Am. Chem. Soc.* **2010**, *132*, 1087. (e) Prokop, K. A.; de Visser, S. P.; Goldberg, D. P. *Angew. Chem., Int. Ed.* **2010**, *49*, 5091. (f) Kojima, T.; Nakayama, K.; Ikemura, K.; Ogura, T.; Fukuzumi, S. *J. Am. Chem. Soc.* **2011**, *133*, 11692.

(29) (a) Morimoto, Y.; Kotani, H.; Park, J.; Lee, Y.-M.; Nam, W.; Fukuzumi, S. *J. Am. Chem. Soc.* **2011**, *133*, 403. (b) Park, J.; Morimoto, Y.; Lee, Y.-M.; Nam, W.; Fukuzumi, S. *J. Am. Chem. Soc.* **2011**, *133*, 5236. (c) Park, J.; Morimoto, Y.; Lee, Y.-M.; Nam, W.; Fukuzumi, S. *Inorg. Chem.* **2011**, *50*, 11612. (d) Morimoto, Y.; Park, J.; Kotani, H.; Lee, Y.-M.; Nam, W.; Fukuzumi, S. *Inorg. Chem.* **2012**, *51*, 10025.

(30) (a) Park, J.; Morimoto, Y.; Lee, Y.-M.; Nam, W.; Fukuzumi, S. *J. Am. Chem. Soc.* **2012**, *134*, 3903. (b) Park, J.; Lee, Y.-M.; Nam, W.; Fukuzumi, S. *J. Am. Chem. Soc.* **2013**, *135*, 5052.

(31) (a) Fukuzumi, S. *Bull. Chem. Soc. Jpn.* **1997**, *70*, 1. (b) Fukuzumi, S. *Org. Biomol. Chem.* **2003**, *1*, 609. (c) Fukuzumi, S. *Bull. Chem. Soc. Jpn.* **2006**, *79*, 177. (d) Fukuzumi, S. *Pure Appl. Chem.* **2007**, *79*, 981.

(e) Fukuzumi, S. *Prog. Inorg. Chem.* **2009**, *56*, 49. (f) Fukuzumi, S.; Ohkubo, K. *Coord. Chem. Rev.* **2010**, *254*, 372.
(32) (a) Fukuzumi, S.; Ohkubo, K. *Chem.—Eur. J.* **2000**, *6*, 4532. (b) Fukuzumi, S.; Yasui, K.; Suenobu, T.; Ohkubo, K.; Fujitsuka, M.; Ito, O. *J. Phys. Chem. A* **2001**, *105*, 10501. (c) Yuasa, J.; Fukuzumi, S. *J. Am. Chem. Soc.* **2006**, *128*, 14281. (d) Yuasa, J.; Yamada, S.; Fukuzumi, S. *J. Am. Chem. Soc.* **2006**, *128*, 14938. (e) Yuasa, J.; Yamada, S.; Fukuzumi, S. *J. Am. Chem. Soc.* **2008**, *130*, 5808. (f) Yuasa, J.; Fukuzumi, S. *J. Phys. Org. Chem.* **2008**, *21*, 886.
(33) (a) Lam, W. W. Y.; Yiu, S.-M.; Lee, J. M. N.; Yau, S. K. Y.; Kwong, H.-K.; Lau, T.-C.; Liu, D.; Lin, Z. *J. Am. Chem. Soc.* **2006**, *128*, 2851. (b) Yiu, S.-M.; Man, W.-L.; Lau, T.-C. *J. Am. Chem. Soc.* **2008**, *130*, 10821. (c) Du, H.; Lo, P.-K.; Hu, Z.; Liang, H.; Lau, K.-C.; Wang, Y.-N.; Lam, W. W. Y.; Lau, T.-C. *Chem. Commun.* **2011**, *47*, 7143.
(34) Fukuzumi, S.; Morimoto, Y.; Kotani, H.; Naumov, P.; Lee, Y.-M.; Nam, W. *Nat. Chem.* **2010**, *2*, 756.
(35) (a) Yocum, C. F. *Coord. Chem. Rev.* **2008**, *252*, 296. (b) Yachandra, V. K.; Yano, J. *J. Photochem. Photobiol. B* **2011**, *104*, 51.
(36) (a) Wiechen, M.; Zaharieva, I.; Dau, H.; Kurz, P. *Chem. Sci.* **2012**, *3*, 2330. (b) Han, X.; Zhang, T.; Du, J.; Cheng, F.; Chen, J. *Chem. Sci.* **2013**, *4*, 368. (c) Park, Y. J.; Cook, S. A.; Sickerman, N. S.; Sano, Y.; Ziller, J. W.; Borovik, A. S. *Chem. Sci.* **2013**, *4*, 717.
(37) Chen, J.; Lee, Y.-M.; Davis, K. M.; Wu, X.; Seo, M. S.; Cho, K.-B.; Yoon, H.; Park, H. J.; Fukuzumi, S.; Pushkar, Y. N.; Nam, W. *J. Am. Chem. Soc.* **2013**, *135*, 6388.
(38) Leeladee, P.; Baglia, R. A.; Prokop, K. A.; Latifi, R.; de Visser, S. P.; Goldberg, D. P. *J. Am. Chem. Soc.* **2012**, *134*, 10397.
(39) (a) Tsui, E.; Y. Tran, R.; Yano, J.; Agapie, T. *Nat. Chem.* **2013**, *5*, 293. (b) Kanady, J. S.; Mendoza-Cortes, J. L.; Tsui, E. Y.; Nielsen, R. J.; Goddard, W. A., III; Agapie, T. *J. Am. Chem. Soc.* **2013**, *135*, 1073.
(40) Kanady, J. S.; Tsui, E. Y.; Day, M. W.; Agapie, T. *Science* **2011**, *333*, 733.
(41) (a) Wu, X.; Seo, M. S.; Davis, K. M.; Lee, Y.-M.; Chen, J.; Cho, K.-B.; Pushkar, Y. N.; Nam, W. *J. Am. Chem. Soc.* **2011**, *133*, 20088. (b) Yoon, H.; Morimoto, Y.; Lee, Y.-M.; Nam, W.; Fukuzumi, S. *Chem. Commun.* **2012**, *48*, 11187.
(42) Evans, D. F.; Jakubovic, D. A. *J. Chem. Soc., Dalton Trans.* **1988**, 2927.
(43) Fukuzumi, S.; Kondo, Y.; Mochizuki, T.; Tanaka, T. J. *Chem. Soc., Perkin Trans. 2* **1989**, 1753.
(44) Kohn, W.; Sham, L. J. *Phys. Rev.* **1965**, *140*, A1133.
(45) A solvent molecule may coordinate to the Sc center. However, a solvent molecule was not incorporated in the present DFT calculations, which were performed to demonstrate that the second Sc^{3+} ion is located at the secondary coordination sphere. The exact structure has yet to be clarified.
(46) The blue-shift in UV−vis indicates an increased energy gap between the HOMO−LUMO orbitals. However, this issue is not directly related to any increase/decrease in E_{red} values, which is a measure of the LUMO orbital energy (not HOMO). The presence of Sc^{3+} can shift the energies of all the orbitals of the $Mn^{IV}O$ moiety (including both HOMO and LUMO orbitals).
(47) (a) Marcus, R. A. *Annu. Rev. Phys. Chem.* **1964**, *15*, 155. (b) Marcus, R. A.; Sutin, N. *Biochim. Biophys. Acta Rev. Bioenerg.* **1985**, *811*, 265. (c) Marcus, R. A. *Angew. Chem., Int. Ed. Engl.* **1993**, *32*, 1111.
(48) Armarego, W. L. F.; Chai, C. L. L. *Purification of Laboratory Chemicals*, 6th ed.; Pergamon Press: Oxford, U.K., 2009.
(49) *Organic Syntheses*; Saltzman, H.; Sharefkin, J. G., Eds.; Wiley: New York, 1973; Vol. *V*, pp 658.
(50) (a) Lubben, M.; Meetsma, A.; Wilkinson, E. C.; Feringa, B.; Que, L., Jr. *Angew. Chem., Int. Ed.* **1995**, *34*, 1512. (b) Duelund, L.; Hazell, R.; McKenzie, C. J.; Nielsen, L. P.; Toftlund, H. *J. Chem. Soc., Dalton Trans.* **2001**, 152. (c) Groni, S.; Dorlet, P.; Blain, G.; Bourcier, S.; Guillot, R.; Anxolabéhère-Mallart, E. *Inorg. Chem.* **2008**, *47*, 3166.
(51) (a) Fussa-Rydel, O.; Zhang, H.-T.; Hupp, J. T.; Leidner, C. R. *Inorg. Chem.* **1989**, *28*, 1533. (b) Fukuzumi, S.; Nakanishi, I.; Tanaka, K.; Suenobu, T.; Tabard, A.; Guilard, R.; Van Caemelbecke, E.; Kadish, K. M. *J. Am. Chem. Soc.* **1999**, *121*, 785.
(52) Frisch, M. J.; et al. *Gaussian 09*, Revision B.01, Gaussian Inc.: Wallingford, CT, 2009.
(53) (a) Becke, A. D. *Phys. Rev. A* **1988**, *38*, 3098. (b) Becke, A. D. *J. Chem. Phys.* **1993**, *98*, 1372. (c) Becke, A. D. *J. Chem. Phys.* **1993**, *98*, 5648. (d) Lee, C.; Yang, W.; Parr, R. G. *Phys. Rev. B* **1988**, *37*, 785.
(54) (a) The LACVP and LACV3P*+ basis sets uses pople style 6-31G and 6-311+G* basis sets (respectively) on all atoms except transition metals, where an ECP is used as defined in the quantum chemistry program Jaguar, version 7.7, Schrödinger, LLC, New York, NY, 2010. See also (b) Hay, P. J.; Wadt, W. R. *J. Chem. Phys.* **1985**, *82*, 299. (c) Dyall, K. G. *Theor. Chem. Acc.* **2004**, *112*, 403.
(55) (a) Barone, V.; Cossi, M. *J. Phys. Chem. A* **1998**, *102*, 1995. (b) Cossi, M.; Rega, N.; Scalmani, G.; Barone, V. *J. Comput. Chem.* **2003**, *24*, 669.